Electronic Supplementary Material (ESI) for Chemical Communications.

SUPPORTING INFORMATION

Ultrasensitive and Highly Selective Detection of Dopamine by NiFeP based Flexible Electrochemical Sensor

Experimental

Materials

The following chemicals were used as received without any further purification. KH_2PO_4, K_2HPO_4, urea and isopropyl alcohol was procured from Merck. Nickel chloride extra pure(hexahydrate) (97% crystalline), red phosphorus 98% crystalline) were purchased from Lobachemie and ferrous sulphate (99.5 % crystalline) was from SDFCL. Dopamine hydrochloride (>99% crystalline), uric acid and ascorbic acid (99% crystalline) were from Sigma-Aldrich and dopamine hydrochloride injections (40 mg mL^{-1}) were purchased from Neon Laboratories Ltd. PBS (0.1 M) was prepared from stock solutions of 0.1 M KH_2PO_4 and 0.1 M K_2HPO_4 and deionized water obtained from a Millipore system (>12 MΩ cm^{-1}).

Synthesis of NiFeP

Synthesis procedure consisting of two steps;

1st step, in a typical synthesis, a mixture of 3:1 molar ratio of $NiCl_2.6H_2O$ and $FeSO_4.7H_2O$ was dissolved under stirring in 35 ml water, then 1.8 g of urea was quickly added and the stirring was continued until homogeneous solution was obtained. Subsequently, the obtained solution was treated at 120 °C for 6 h using Teflon-lined autoclave. Brown colour $NiFe(OH)_2$ was obtained which was tharoughly washed with water and ethanol several times to remove the impurities and dried overnight at 60 °C.

2nd step: Resulted nickel iron layer double hydroxides was mixed with 100 mg of red phosphorous in 10 ml water and was subjected to microwave-assisted reactions using Muiltiwave Pro instrument from Anton Paar. Before irradiation, N_2 gas was purged into reaction mixture for 10 min. The sample was irradiated at 100 °C with a 15 min ramp and holding for 30 min at 100 °C, under a limiting pressure of 18 bar at 600 watt by controlled temperature programming. Obtained precipitate was filtered and washed 2-3 times with deionised water and dried at 60 °C in an oven.

Similarly, NiP_x was synthesised under smilar reaction conditions as above using only $NiCl_2.6H_2O$ metal salt and rest remains the same. While FeP_x was syntheised similar to NiFeP, expect the addition of $NiCl_2.6H_2O$ in the synthesis process.

For the synthesis of NiO_x, initially aqueous solution $NiCl_2.6H_2O$ and urea (1:2) was prepared and transferred into 50 mL Teflon-lined autoclave and treated at 120 °C for 6 h resulted in $Ni(OH)_2$ is obtained. Further, by thermal decom-position of $Ni(OH)_2$ at 300 °C for 2 h gives NiO nanoparticles. As obtained material was filtered and washed 2-3 times using deionised water then dried at 60 °C in an oven. Synthesis procedure for FeO_x was similar to NiO_x, using only $FeSO_4.7H_2O$ in the synthesis process.

Physical characterization

The microstructure of the syntheised catalysts were characterized using X-ray powder diffraction (XRD by PANalytical X'PERT pro diffractometer using Cu *Kα* radiation (λ=0.1542 nm, 40Kv, 40mA). The diffraction pattern was recorded in the 2θ range of 5-80° with a scan speed of 2° per minute. The morphology of the catalysts were performed by field emission scanning microscopy (FESEM) (ZEISS Ultraplus - 4095) and transmission electron microscopy (TEM). The high resolution TEM (HR-TEM) images were recorded usig a JEM 2100 (JEOL, Japan) operating at 200 keV. The oxidation state of the syntheised catalysts were anlaysed by X-ray photoelectron spectroscopy (XPS) using PHI 5000 Versa Prob II spectrometer using Al *Kα* radiation (1486.6 eV) working at 15 kV and 35 mA under an ultrahigh vacuum (UHV; 7×10^{-10} mbar pressure). The spectra were calibrated with respect to C (1s) peak at 284.5 eV with a precision of ±0.2 eV.

Electrochemical measurements

All the electrochemical measurements were performed using electrochemical workstation (Bio-Logic (VSP 300)) with standard three electrode system in a single compartment cell, in which catalyst modified glassy carbon electrode (Ø3 mm) used as working electrode (WE), Pt wire as counter electrode (CE), Ag/AgCl/3MKCl as reference electrode (RE). Before each analysis, GC was polished on nylon polishing cloths (SM 407052, AKPOLISH) by employing different grades of alumina slurry (3, 0.3, 0.05 µm PINE instrument, USA) followed by thorough washing and ultrasonication to remove an adsorbed impurities and alumina particles. The NiFeP catalyst slurry was prepared by dispersing 1.25 mg of the catalyst in 0.5 ml of solution containing isopropyl alcohol and Millipore water with a volume ratio of 4:1 by ultrasonicating for 30 min to form a homogeneous ink. Then 20 µL (50 µg) of the as-prepared slurry was drop-casted on the GC electrode for electrocatalytic activity measurements and dried at room temperature.

Electrochemical impedance measurements were conducted at a DC voltage of 210 mV over a frequency range between 10 mHz to 3 MHz. Each experiment has been performed at least 5 times to ensure reproducibility.

Fabrication of flexible paper electrode

Flexible paper electrodes were prepared by simple drop casting method, in which NiFeP catalyst slurry (detailed in the above section) was drop coated onto Whatman filter paper (1.1 mm thickness) and was dried at room temperature. The process of fabrication is shown in scheme S1 wherein, NiFeP catalyst coated Whatman filter paper serves as binder free flexible working electrode with an area of 1.53 cm^2 and the contact was made through the Cu wire using Ag-paste and sealed with Teflon tape as shown in scheme for electrochemical measurement.

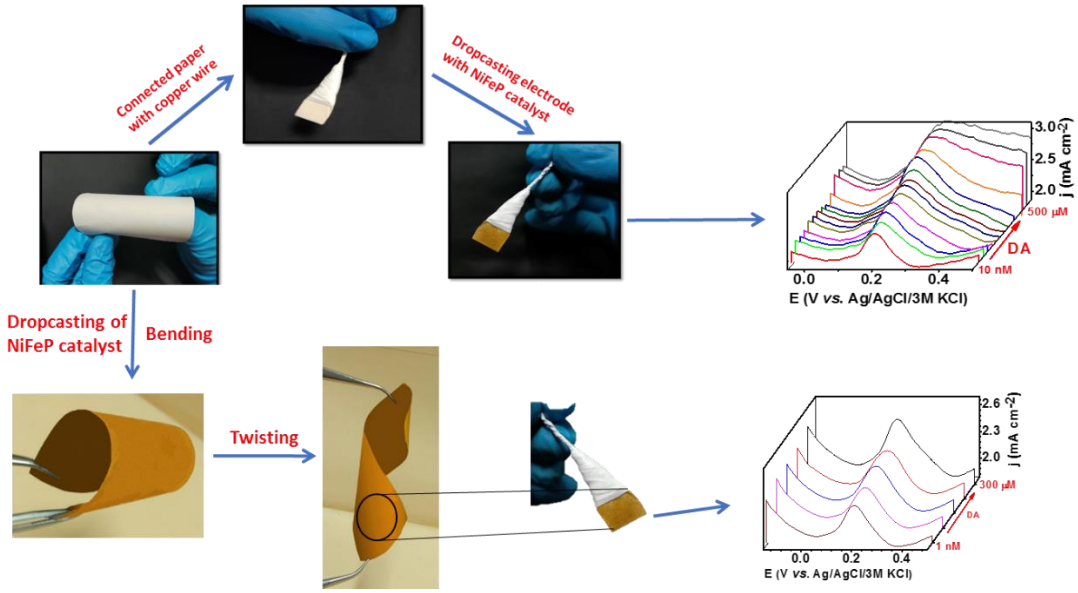

Scheme S1: Schematic representating the fabrication of paper electrode and its activity before and after the deformation of the electrode.

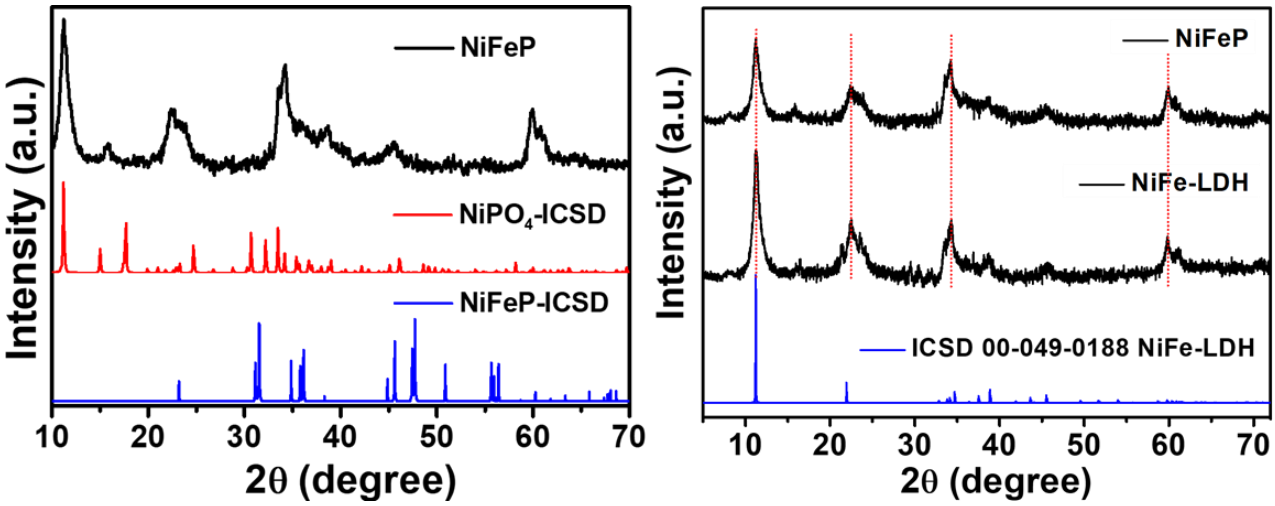

Figure S1. XRD pattern of NiFeP and NiFe-LDH catalyst along with ICSD profiles.

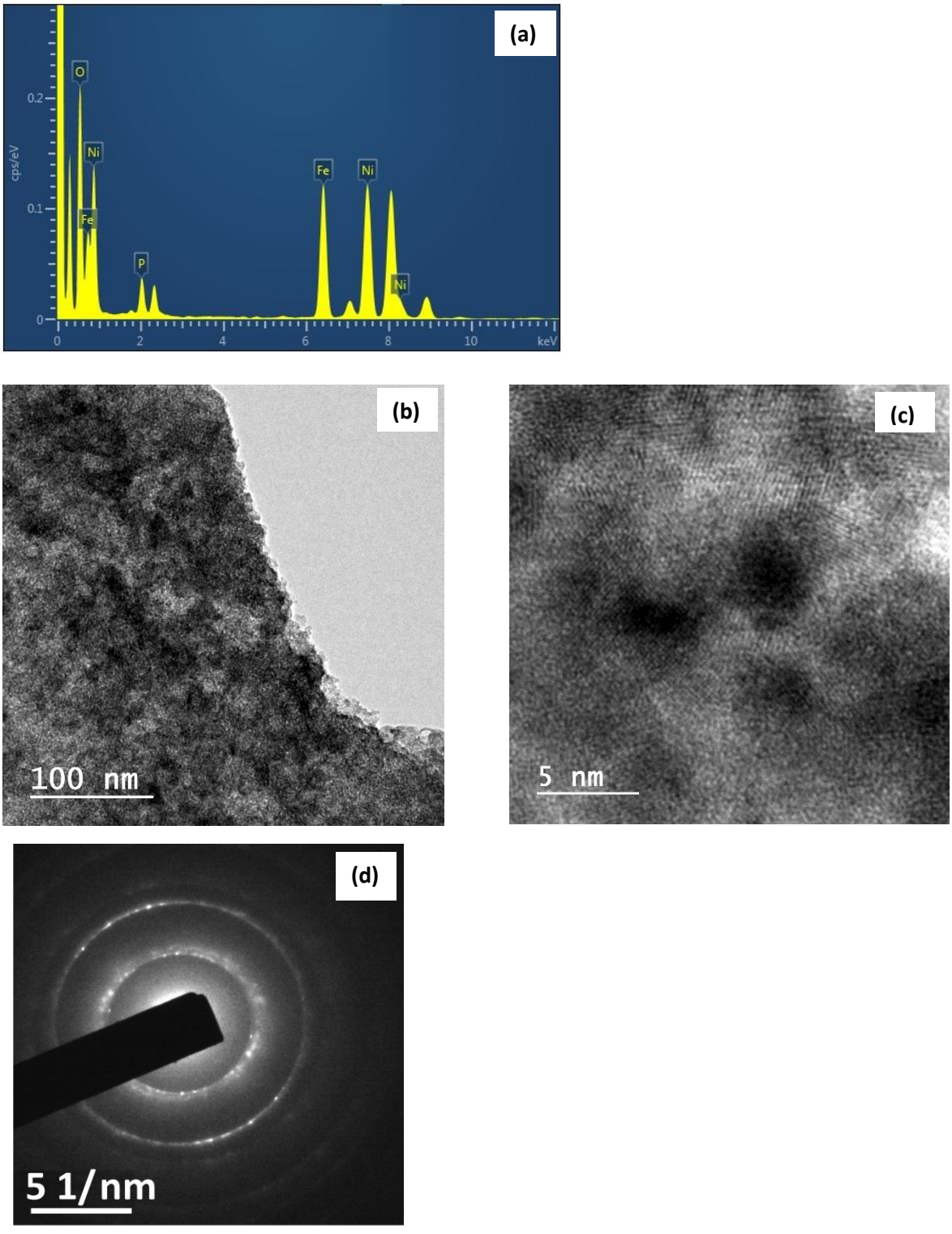

Figure S2. (a) EDS spectrum, (b) TEM, (c) HRTEM and (d) SAED pattern of NiFeP catalyst.

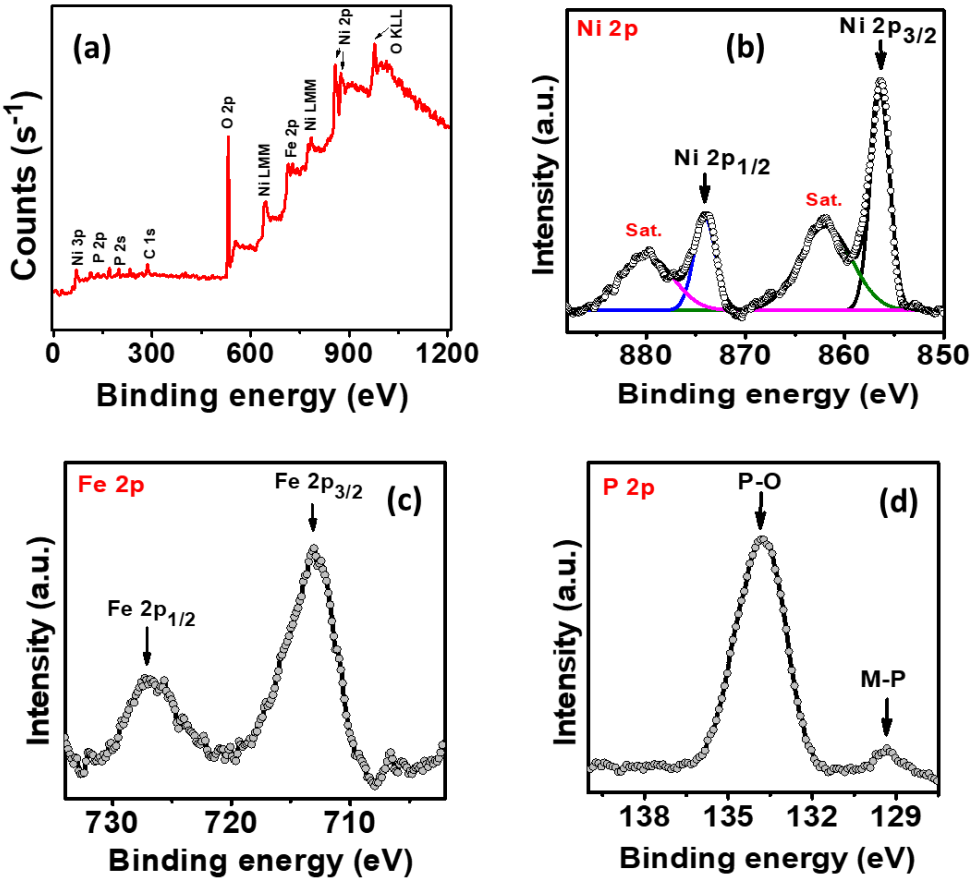

Figure S3. (a) XP survey spectra of NiFeP catalyst, (b) XP spectra of Ni 2p, (c) Fe 2p and (d) P 2p of NiFeP catalyst.

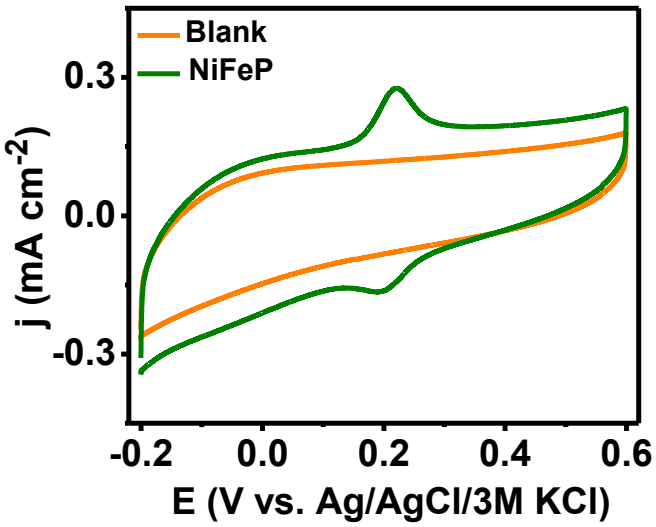

Figure S4. (a) Cyclic voltammogram of NiFeP in 0.1 M PBS electrolyte with 50 µM DA and 200 µM AA and without DA(Blank) at a scn rate of 50 mV s^{-1}; CE: Pt wire, RE: Ag/AgCl/3 M KCl.

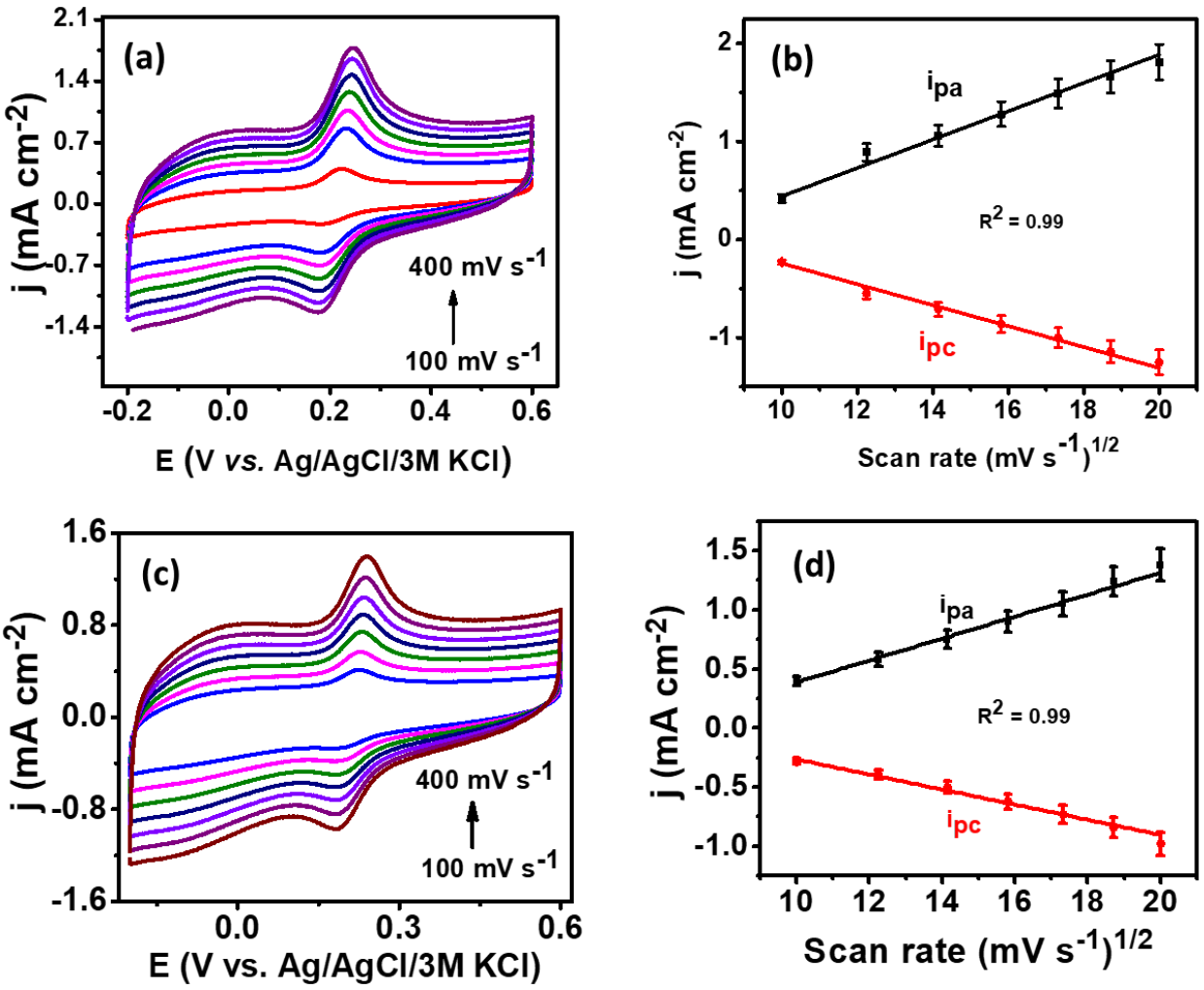

Figure S5. Cyclic voltammograms of NiFeP over GCE in 0.1 M PBS (pH 7.0) electrolyte containing (a) 400 µM DA and 200 µM AA and (b) 50 µM DA and (200 µM AA) respectively at various scan rates ranging from 100 to 500 mV s^{-1}, (b) and (d) corresponding average current density versus scan rate CE: Pt wire, RE: Ag/AgCl/3 M KCl.

Electrochemical surface area (ECSA)

Electrochemical active surface area of catalyst was determined by computing the double-layer pseudo-capacitance (C_{dl}) in 0.1 M PBS along with analyte solution. Cyclic voltammetry was performed in non-faradic region /double-layer region in potential range from -0.2 V to 0.16 V *vs.* Ag/AgCl/3 M KCl at various scan rates (50 to 500 mV/s). The slope of the plot between averaged current density of both anodic and cathodic current $(I_a+I_c)/2$ ('a' denotes anodic current and 'c' is for cathodic current) versus the scan rate at -0.08 V *vs.* Ag/AgCl/3 M KCl gives pseudo-capacitance (C_{dl}). As obtained C_{dl} was dividing with the specific capacitance of the flat standard surface (20-60 µF cm^{-2}) which in the present study is considered to be 40 µF cm^{-2}, gives electrochemical surface area (ECSA). The roughness of the surface was further calculated by dividing the obtained ECSA with the geometrical surface area.

ECSA calculation:[16]

ECSA = C_{dl} / Cs; where Cs is specific capacitance.

Roughness factor (a.u.) = ECSA / geometrical surface area

where geometrical surface area is 0.0707 cm^{-2}

Table S1: Electrochemical surface area (ECSA) determination.

S. No.	Catalyst	Electrolyte	C_{dl}*(µF) at -0.08 V	ECSA (cm^2)	Roughness factor (a.u.)
1	NiP_x	50 µM DA + 200 µM AA + 0.1 M PBS	1.35	0.033	0.47
2	FeP_x	50 µM DA + 200 µM AA + 0.1 M PBS	2.78	0.069	0.98
3	NiO_x	50 µM DA + 200 µM AA + 0.1 M PBS	1.92	0.048	0.67
4	FeO_x	50 µM DA + 200 µM AA + 0.1 M PBS	3.04	0.076	1.07
5	NiFeP	50 µM DA + 200 µM AA + 0.1 M PBS	52.1	1.3	18.42
6	NiFeP	400 µM DA + 200 µM AA + 0.1 M PBS	77.77	1.94	27.5

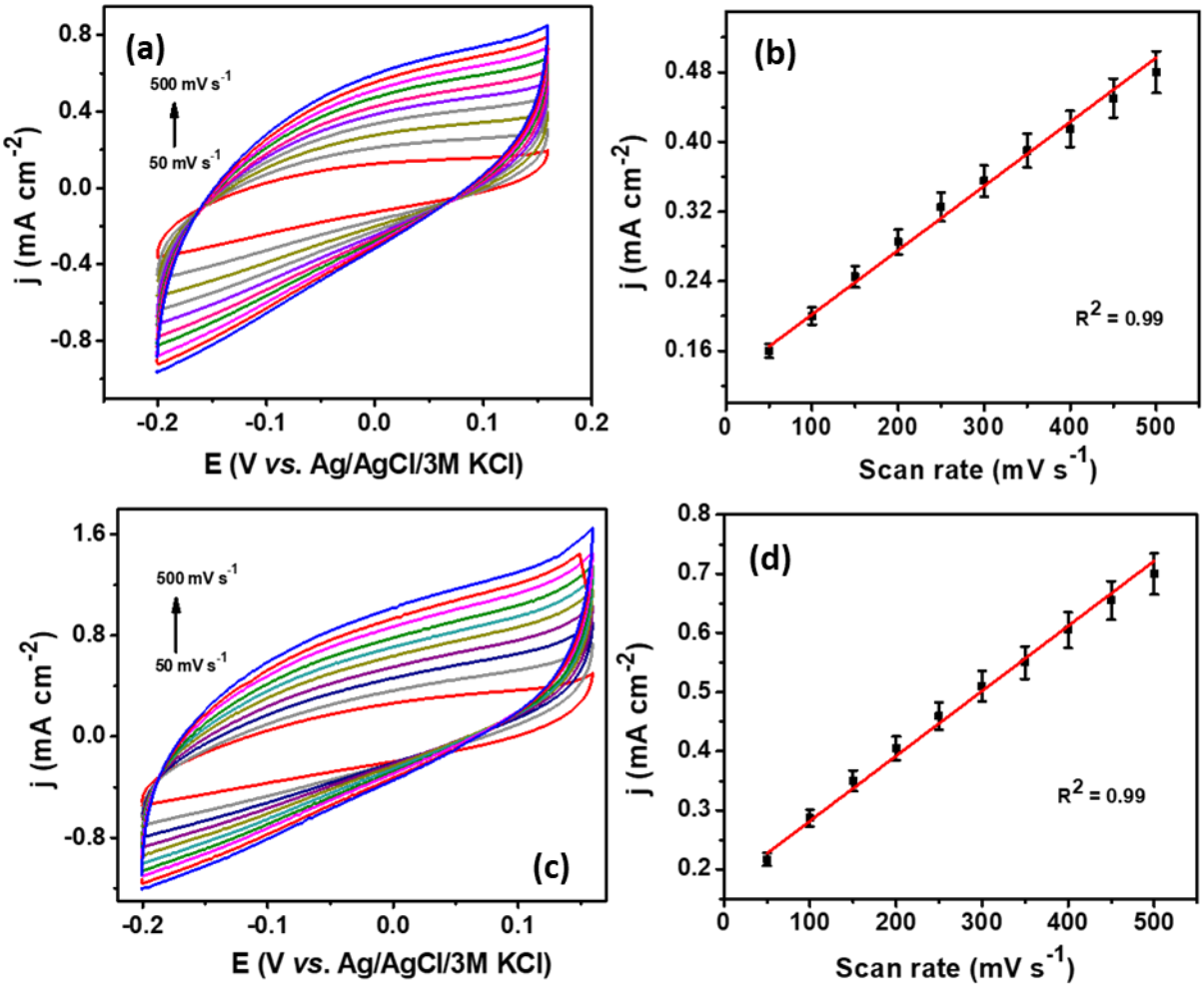

Figure S6. Cyclic voltammograms of NiFeP over GCE in 0.1 M PBS (pH 7.0) electrolyte containing 200 μM AA and (a) 50 μM DA, (c) 400 μM DA in non-faradic potential region and (b &d) corresponding average current density versus scan rate at various scan rates ranging from 50 to 500 mV s^{-1}. CE: Pt wire, RE: Ag/AgCl/3M KCl.

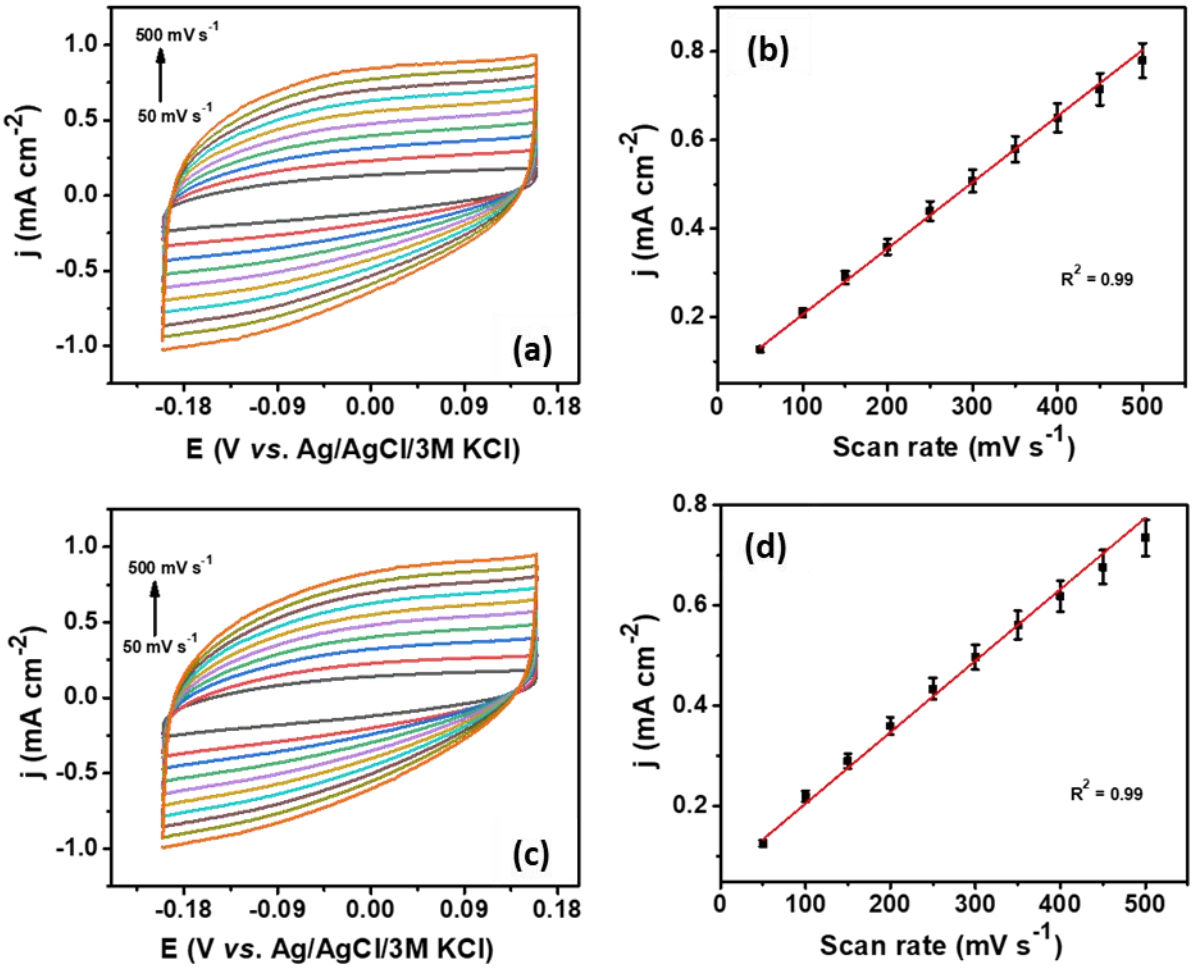

Figure S7. Cyclic voltammograms of (a) NiP_x and (c) FeP_x catalyst at varying scan rates in the non-faradic potential region and (b & d) corresponding average current density respectively versus scan rate at various scan rates ranging from 50 to 500 mV s^{-1}. CE: Pt wire, RE: Ag/AgCl/3M KCl.

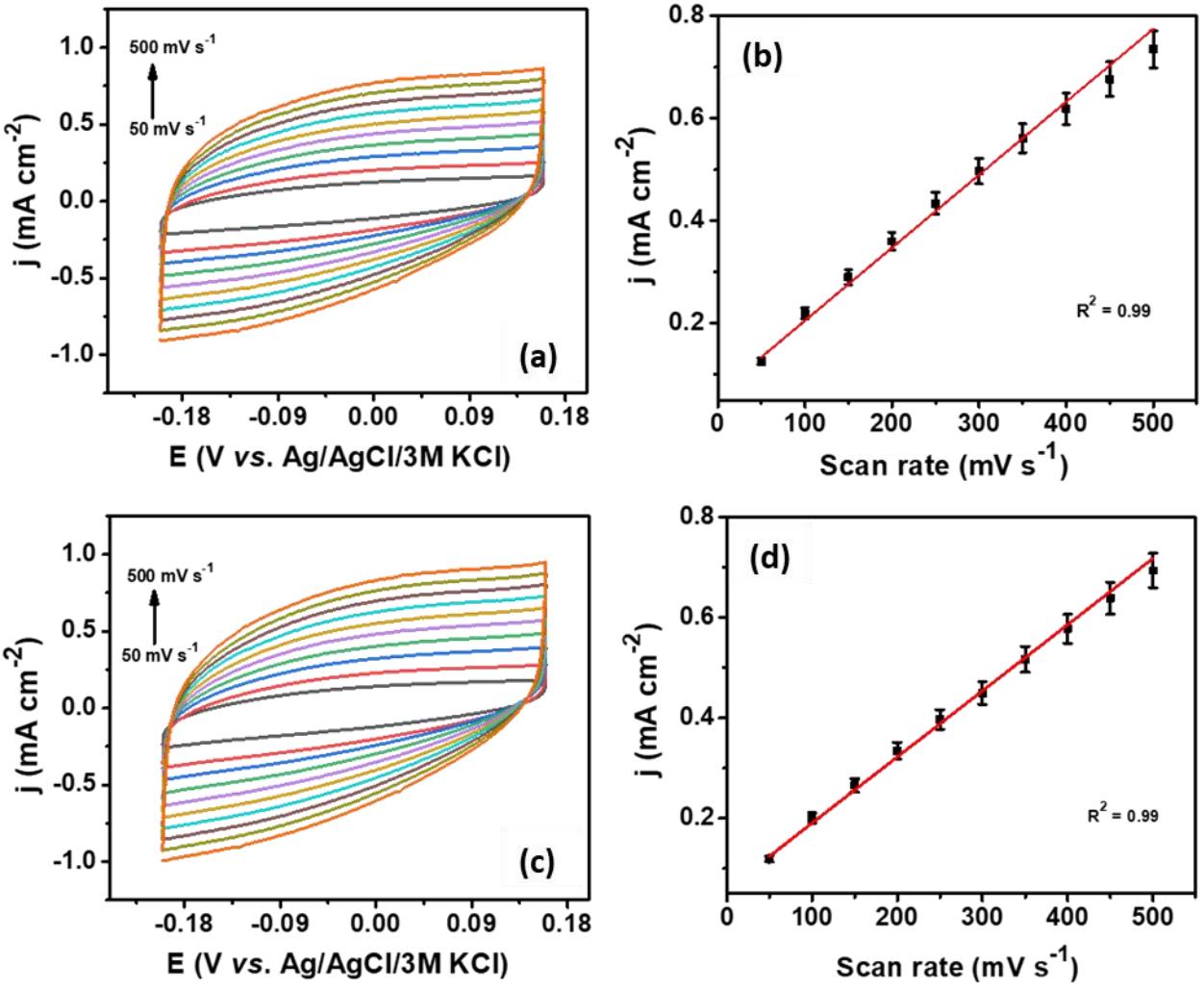

Figure S8. Cyclic voltammograms of (a) NiO_x and (c) FeO_x at varying scan rates in the non-faradic potential region and (b & d) corresponding average current density respectively versus scan rate at various scan rates ranging from 50 to 500 mV s^{-1}. CE: Pt wire, RE: Ag/AgCl/3M KCl.

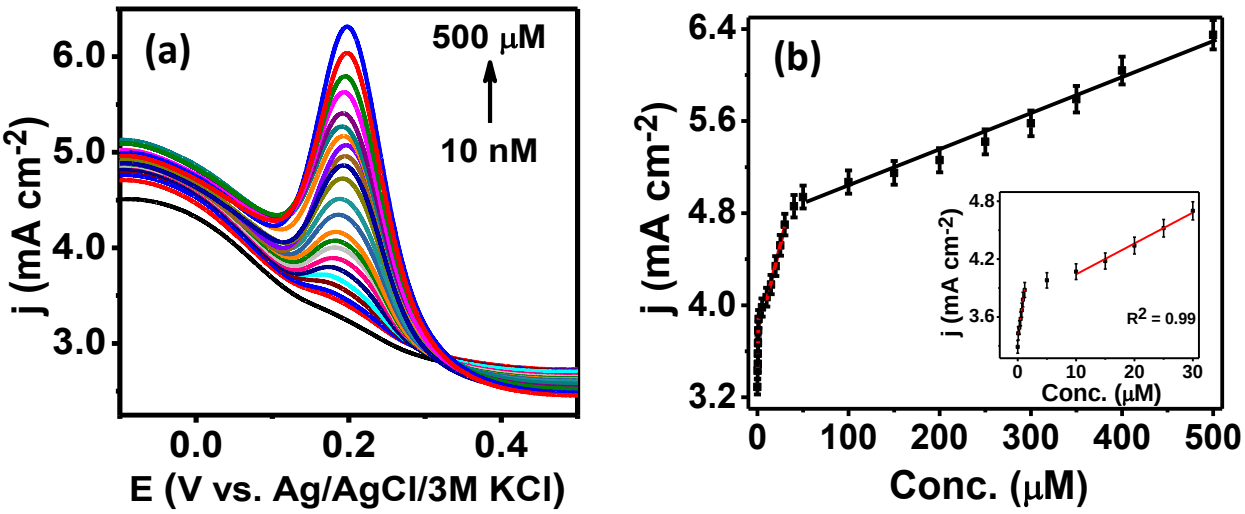

Figure S9. (a) SWV of NiFeP catalyst in 0.1 M PBS (pH 7.0) electrolyte at various concentrations of DA, step height of 0.7 mV, pulses width of 32 ms, CE: Pt wire, RE: Ag/AgCl/3M KCl.
(b) Plot of current density versus concentration of DA for NiFeP catalyst extracted from SWV.

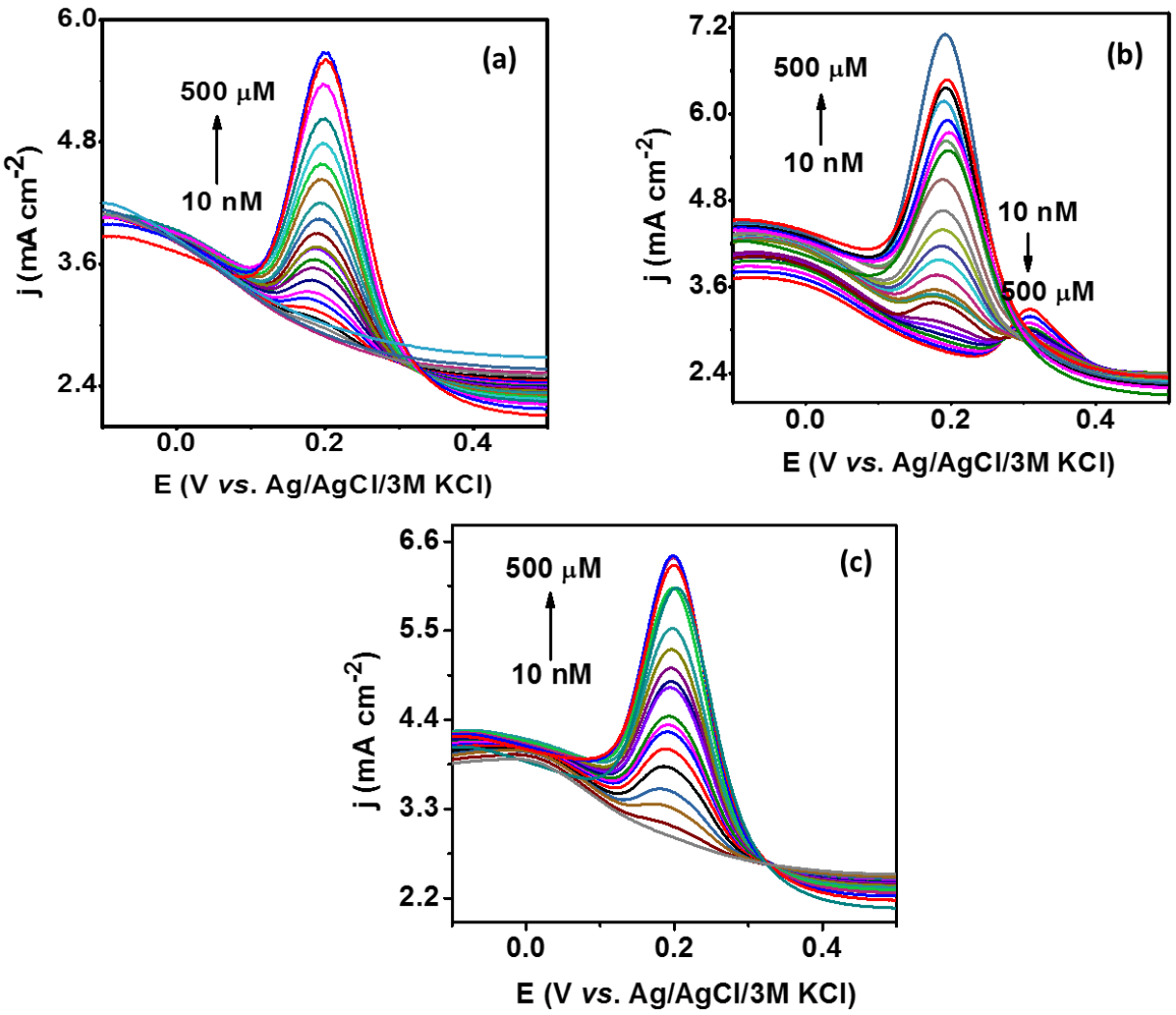

Figure S10. Square wave voltammogram of NiFeP over GCE in presence of interferants (a) 3000 μM glucose, (b) 200 μM UA and (c) 1000 μM AA in 0.1 M PBS (pH 7.0) electrolyte at various concentrations of DA, step height of 0.7 mV, pulses width of 32 ms, CE: Pt wire, RE: Ag/AgCl/3M KCl.

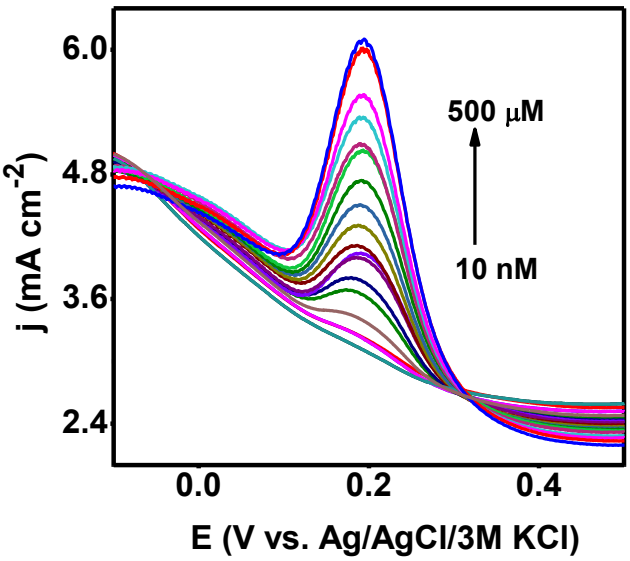

Figure S11. SWV of NiFeP over GCE in 0.1 M PBS (pH 7.0) electrolyte containing various concentrations of only DA, step height of 0.7 mV, pulses width of 32 ms CE: Pt wire, RE: Ag/AgCl/3M KCl.

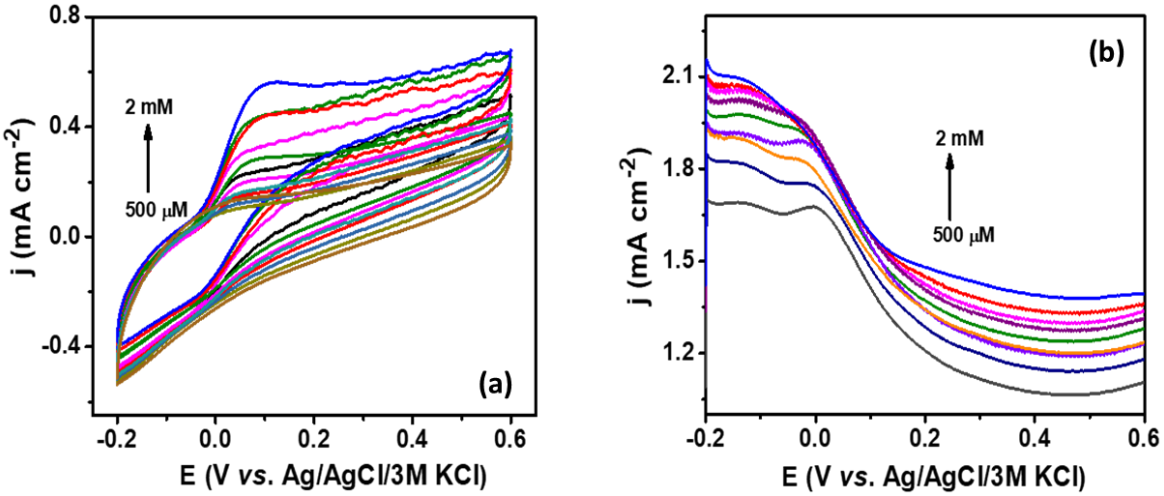

Figure S12. (a) CV, (b) SWV of NiFeP over GCE in 0.1 M PBS (pH 7.0) electrolyte containing various concentrations of only AA, step height of 0.7 mV, pulses width of 32 ms, CE: Pt wire, RE: Ag/AgCl/3M KCl.

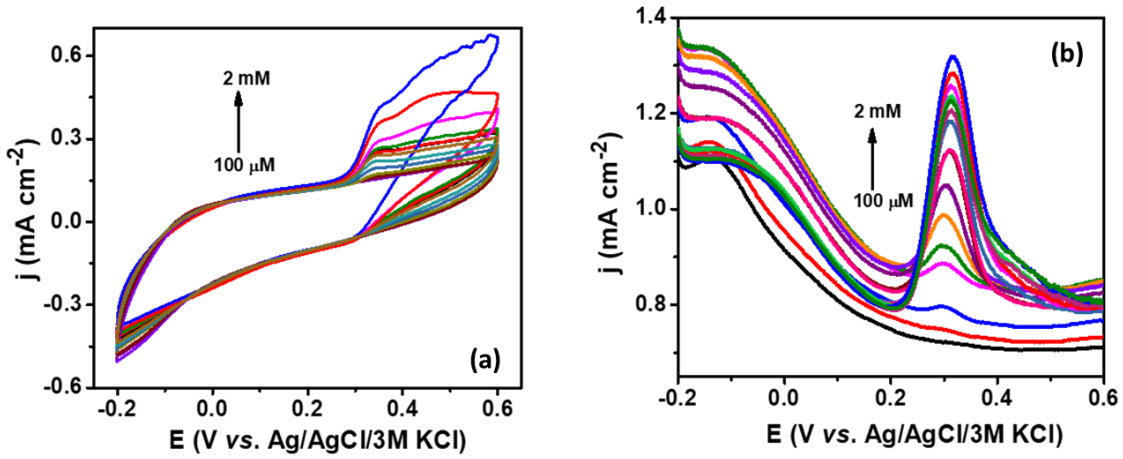

Figure S13. (a) CV, (b) SWV of NiFeP over GCE in 0.1 M PBS (pH 7.0) electrolyte containing various concentrations of only UA, step height of 0.7 mV, pulses width of 32 ms CE: Pt wire, RE: Ag/AgCl/3M KCl.

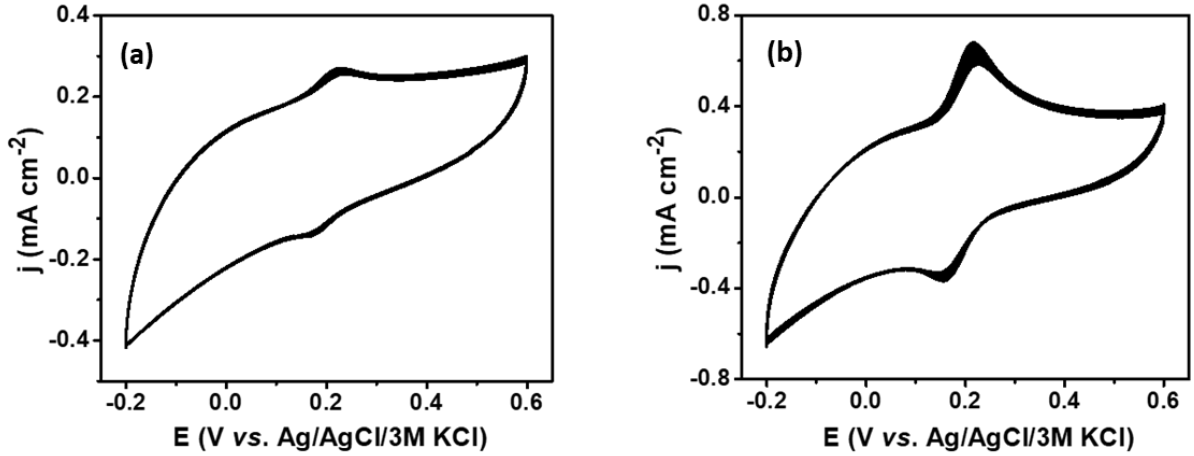

Figure S14. Cyclic voltammograms of NiFeP over GCE in 0.1 M PBS (pH 7.0) electrolyte containing (a) 50 µM DA and 200 µM AA, (b) 500 µM DA and 200 µM AA for 100 cycles at a scan rate of 50 mV s^{-1}, CE: Pt wire, RE: Ag/AgCl/3 M KCl.

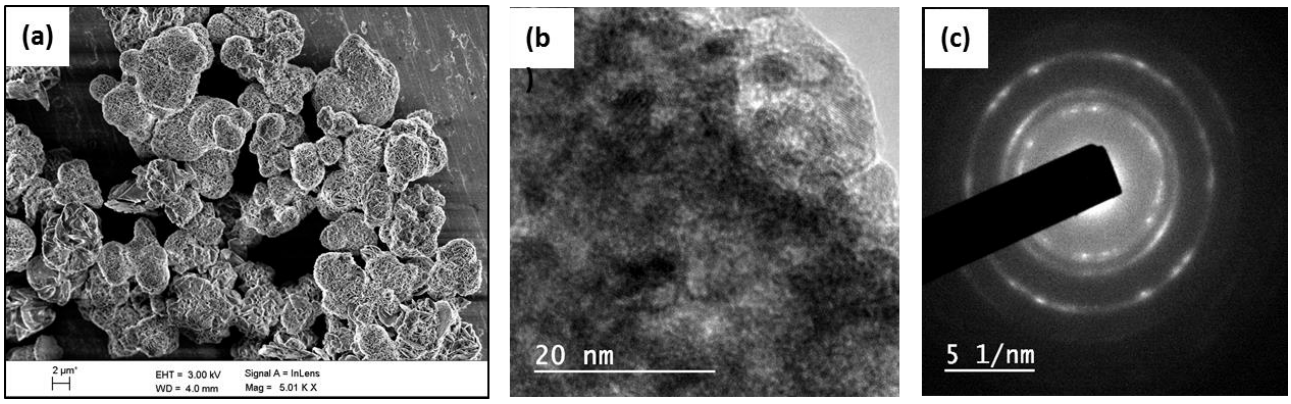

Figure S15. (a) FE-SEM, (b) HRTEM images and (c) SAED pattern for NiFeP catalyst after 100 CV cycling in 0.1 M PBS electrolyte containg 500 µM DA and 200 µM AA at a scan rate of 50 mV s^{-1}, CE: Pt wire, RE: Ag/AgCl/3 M KCl.

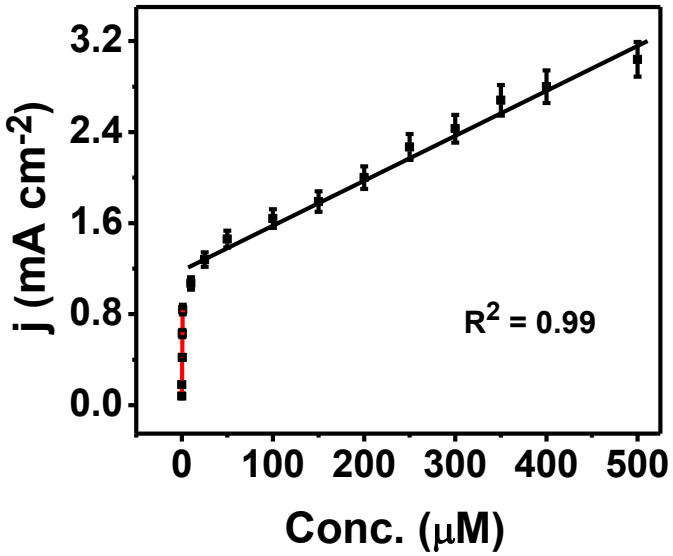

Figure S16. Plot of current density versus concentration of DA for NiFeP catalyst over flexibale paper electrode extracted from SWV Figure 3a.

Furthermore, in order to validate the applicability of the proposed sensor in practical applications for the detection of DA, NiFeP catalyst was analyzed in real sample using commercially available DA hydrochloride injections (40 mg mL^{-1}) via standard addition method. Injection was diluted to a concentration of 5 μM using PBS (0.1 M, pH 7.0) and known amounts of DA in the test solution was added. The obtained results are tabulated in Table S2 (SI). The recovery of the spiked sample ranges from 97 to 108, which ascertain the applicability of the proposed sensor for real time application as well.

Table S2. Analytical results of NiFeP modified glassy carbon electrode towards determination of dopamine from commercially available dopamine hydrochloride injection.

Sample	**Actual Conc.**	**Conc. (Added)**	**Conc. (found)**	**Recovery (%)**
1.	5 μM	5 μM	10.8	108
2.	5 μM	10 μM	14.6	97.3

Table S3. Comparison of analytical performance of DA sensor with various modified electrodes reported previously

Electrode	**Linear range (μM)**	**Lowest detection limit (μM)**	**Sensitivity value (μA μM^{-1} cm^{-2})**	**Ref.**
SGPGENa	0.15–45	0.0082	20.81	1
Fe_2O_3-erGO /GCE	0.25-100	0.024	12.56	2
CS film/ZnO NPs@C/3D-KSC	0.00012-152	0.000039	0.757	3
Ag/MoS_2	0.2-50	0.2	-	4
PT/Au/CNT-4.5	1.0–10	0.69	19.492 μA μM^{-1}	5
Au@Fe_3O_4/GC	0-0.8	0.0027	0.120 μA μM^{-1}	6
Nf-Ag@HCS/GCE	3-2000 2000-7000	0.6	0.7574 0.3154	7
Nafion/Pt/MC/GCE	0.1-193	0.034	0.01223 μA μM^{-1}	8
$FeTiO_3$	1-90 110-350	0.0013	1.56	9
rGO/Bi_2S_3/GCE	0.01-40	0.0123	2.046 μA μM^{-1}	10
rGO-poly(FeTFPP)/GCE	0.05-300	0.023	0.039 μA μM^{-1}	11
Mo NPs@*f*-MWCNTs	0.01-1609	0.00126	4.925	12
CuO/g-C_3N_4	0.2-16.0 16.0-78.7	0.06	0.834 and 0.331	13
poly-β-CD (f-MWCNTs/ PANI/GCE	2 - 24	0.0164	26.79	14
NW/PET	0.2-600	0.026	0.178	15
PEDOT-PB	30 to 90	8.23	0.116 μA μM^{-1}	16
GNB/GCE	2-200	0.58	0.95	17
ERGO/GCE	0.5-60	0.5	0.482 μA μM^{-1}	18
PEDOT modified laser scribed graphene	1-150	0.33	0.220 ± 0.011 μA μM^{-1}	19
pyrolytic carbon film (PCF) electrode		0.04	5.345 A M^{-1}	20
Ni-V_2O_5/GCE	6.6-96.4	0.028	0.132 μA μM^{-1}	21
CB-Chit	0.1-1400	0.1	1.88	22
MoS_2 NSB/CNFs	1-60	0.04	6.24	23
Au@Pt/GO/GCE	0.5-177.5	0.11	0.329	24
GO-MWCNT/MnO_2/ AuNP/ GCE	0.5-2500	0.17	0.2334	25
rGO/Pd/GCE	1-150	0.233	2.62	26
3D N-doped graphene	3-100	0.001	9.87	27
rGO/TiO_2{001}/GCE	2-60	6		28
MnS/GO/GCE	0.04-138.07	0.007	3.11	30
PVIM−Cobalt polyoxometalate/CNT	0.0005-600	0.0005 (500 pM)		29
NiFeP	**0.01-500**	**0.0003** (300 pM)	**427 (solid electrolde)** **756 (paper electrode)**	**This Work**

References

1. X. Fan, Y. Xu, T. Sheng, D. Zhao, H. Yuan, F. Liu, X. Liu, X. Zhu, L. Zhang and J. Lu, *Microchim. Acta*, 2019, **186**, 324.
2. G. Mathew, P. Dey, R. Das, S. D. Chowdhury, M. P. Das, P. Veluswamy, B. Neppolian and J. Das, *Biosens. Bioelectron.*, 2018, **115**, 53-60.
3. Y. Song, J. Han, L. Xu, L. Miao, C. Peng and L. Wang, *Sens. Actuators, B*, 2019, **298**, 126949.
4. J.-W. Shin, J. Yoon, M. Shin and J.-W. Choi, *Biotechnol. Bioprocess Eng.*, 2019, **24**, 135-144.
5. C. S. Inagaki, M. M. Oliveira, M. F. Bergamini, L. H. Marcolino-Junior and A. J. Zarbin, *J. Electroanal. Chem.*, 2019, **840**, 208-217.
6. A. Thamilselvan, P. Manivel, V. Rajagopal, N. Nesakumar and V. Suryanarayanan, *Colloids Surf., B*, 2019, **180**, 1-8.
7. X. Zhang and J. Zheng, *Sens. Actuators, B*, 2019, **290**, 648-655.
8. X. Li, A. Tian, Q. Wang, D. Huang, S. Fan, H. Wu and H. Zhang, *Int. J. Electrochem. Sci.*, 2019, **14**, 1082-1091.
9. T. Aparna and R. Sivasubramanian, *Mater. Chem. Phys.*, 2019, **233**, 319-328.
10. X. Yan, Y. Gu, C. Li, B. Zheng, Y. Li, T. Zhang, Z. Zhang and M. Yang, *Sens. Actuators, B*, 2018, **257**, 936-943.
11. X. Yan, N. Lu, Y. Gu, C. Li, T. Zhang, H. Liu, Z. Zhang and S. Zhai, *Talanta*, 2018, **179**, 401-408.
12. M. Keerthi, G. Boopathy, S.-M. Chen, T.-W. Chen and B.-S. Lou, *Sci. Rep.*, 2019, **9**, 1-12.
13. Y. Huang, Y. Tan, C. Feng, S. Wang, H. Wu and G. Zhang, *Microchim. Acta*, 2019, **186**, 10.
14. Y. H. Chang, P. M. Woi and Y. Alias, *Microchem. J.*, 2019, **148**, 322-330.
15. M.-S. Hsu, Y.-L. Chen, C.-Y. Lee and H.-T. Chiu, *ACS appl. mater. interfaces*, 2012, **4**, 5570-5575.
16. S. Lupu, C. Lete, M. Marin, N. Totir and P. C. Balaure, *Electrochim. Acta*, 2009, **54**, 1932-1938.
17. P. K. Kannan, S. A. Moshkalev and C. S. Rout, *Nanotechnology*, 2016, **27**, 075504.
18. L. Yang, D. Liu, J. Huang and T. You, *Sens. Actuators, B*, 2014, **193**, 166-172.
19. G. Xu, Z. A. Jarjes, V. Desprez, P. A. Kilmartin and J. Travas-Sejdic, *Biosensors and Bioelectronics*, 2018, **107**, 184-191.
20. M. Hadi and A. Rouhollahi, *Anal. Chim. Acta*, 2012, **721**, 55-60.
21. R. Suresh, K. Giribabu, R. Manigandan, S. P. Kumar, S. Munusamy, S. Muthamizh, A. Stephen and V. Narayanan, *Sens., Actuators B*, 2014, **202**, 440-447.
22. B. Dinesh, R. Saraswathi and A. S. Kumar, *Electrochim. Acta*, 2017, **233**, 92-104.
23. H. Y. Yue, P. F. Wu, S. Huang, Z. Z. Wang, X. Gao, S. S. Song, W. Q. Wang, H. J. Zhang and X. R. Guo, *Microchim. Acta*, 2019, **186**, 378.
24. Z. Yang, X. Liu, X. Zheng and J. Zheng, *J. Electroanal. Chem.*, 2018, **817**, 48-54.
25. D. Rao, X. Zhang, Q. Sheng and J. Zheng, *Microchim. Acta*, 2016, **183**, 2597-2604.
26. S. Palanisamy, S. Ku and S.-M. Chen, *Microchim. Acta*, 2013, **180**, 1037-1042.
27. X. Feng, Y. Zhang, J. Zhou, Y. Li, S. Chen, L. Zhang, Y. Ma, L. Wang and X. Yan, *Nanoscale*, 2015, **7**, 2427-2432.
28. G. T. S. How, A. Pandikumar, H. N. Ming and L. H. Ngee, *Sci. rep.*, 2014, **4**, 5044.
29. N. Thakur, S. D. Adhikary, M. Kumar, D. Mehta, A. K. Padhan, D. Mandal and T. C. Nagaiah, *ACS Omega*, 2018, **3**, 2966-2973.
30. S. Ramki, K. Pandi, S.-M. Chen, Y.-T. Ye, T.-W. Chen and Q. Hao, *Int. J. Electrochem. Sci*, 2019, **14**, 1069-1081.